

EVALUATION OF THE NEW OPERATIONAL FRENCH RADAR PRODUCT

P14.8

FOR URBAN HYDROLOGY

I. Emmanuel^{1*}, P. Tabary², H. Andrieu¹

¹ Laboratoire Central des Ponts et Chaussées, Division Eau, Bouguenais, France

² Centre de Météorologie Radar, Météo France, Toulouse, France

1. INTRODUCTION

Population density and urban extension are factors that make cities vulnerable to floods and pollution. So, the regulation of rivers and retention basins become a strong thematic issue. In such a context, the use of radar images as hydrological model input appears as a major scientific challenge of a great public interest. An accurate management of urban rain waters, including flood warning, requires first to measure rainfall in real-time with a good accuracy then to simulate the hydrological behaviour of urban catchments at temporal and spatial resolutions consistent with the response time of urbanized catchments, usually less than one hour. Typical rain gauge networks are not dense enough to provide the required resolution while rainfall estimations, coming from weather radar systems, are characterized by high space-time resolution (order of km² and few minutes) and can potentially provide this essential information. However, before using radar data as model input, it is necessary to evaluate its sturdiness. The aim of this study is to carry out a critical analysis of the French new radar product (Tabary, 2007) by comparing data from rain gauges to the one measured by the weather radar of Trappes, located in the Paris region, for time steps of 5, 15, 30 and 60 min, according to the distance from the radar, the quality of the radar measurement, the rainfall type and the adjustment factor. A special emphasis is addressed to evaluate the errors inherent to rain gauges (instrumental and representativeness).

* Corresponding author address: Isabelle Emmanuel, LCPC Nantes, Division Eau, BP 4129, 44341 Bouguenais Cedex; e-mail: isabelle.emmanuel@lcpc.fr

2. DATA SET

2.1 Radar data

The Radar data is the new quantitative precipitation estimation product developed by Meteo France. It is measured by the C-band radar of Trappes located 30 km south-west of Paris. This radar is one of the 24 radars of the French operational radar network named "Application Radar à la Météorologie Infra-Synoptique" (ARAMIS). In its studied version the doppler character of this radar is kept aside. The scanning strategy of this radar has been designed specifically for hydrological purposes and currently consists of three successive volume scans. Each volume scan lasts 5 min and is constituted of 6 elevation angles: the three lowest (0.4, 0.8 and 1.5°) are contained in the three scans and therefore are repeated every 5 min; the upper ones differ from one scan to another and are mostly used to identify Vertical Profiles of Reflectivity (VPR). In addition to the Cartesian (512*512 km, 1 km² in resolution) radar rainfall product, a map of quality indicators is automatically generated and allows for assessing empirically the accuracy of the radar estimation. An indicator of 0 is bad whereas an indicator of 100 is excellent. Those indicators take into account the fact that the quality of measurements decreases when the altitude of the radar beam increases and when beam blocking increases.

The rainfall product comprises 8 successive processing steps (Tabary, 2007; Tabary *et al.*, 2007):

- 1-the dynamic identification of ground clutter based on the pulse to pulse fluctuation of the radar signal;
- 2-the reflectivity to rain rate conversion using the Marshall-Palmer Z-R relationship;

3-the correction for partial beam blocking using numerical simulations of the interaction between radar wave and the ground;
 4-the correction for VPR effects based on ratio curves and a priori climatology based VPR candidates;
 5-the correction for nonsimultaneity of radar measurements by making use of a cross-correlation advection field;
 6-the weighted linear combination of the corrected reflectivity measurements gathered at various elevation angles of the volume coverage pattern;
 7-the production of a 5 min rain accumulation using the advection field to mitigate undersampling effects;
 8-the basic adjustment of those 5 min rain accumulation by computing every hour an adjustment factor from rain gauge and radar data (this factor being applied to the entire image during the next hour). The main goal of this step is to overcome potential problems linked to radar calibration but not to treat physical problems. Indeed the principal errors, except attenuation, have already their own correction procedure.

2.2 Rain gauge data

The reference rainfall data is provided by 87 tipping bucket rain gauges located from 0 to 135km around the weather radar of Trappes. The data was of 6 min data but has been converted to 5 min data according to the following basic redistribution:

$$0600_{dt=5min} = 5/6 * 0600_{dt=6min}, \quad (1)$$

$$0605_{dt=5min} = 1/6 * 0600_{dt=6min} + 4/6 * 0606_{dt=6min},$$

etc...

For small time steps, the representativeness problem between rain gauge and radar data is important (precipitation drift, difference between the sampling volumes ...).

2.3 Selected rain events

A total of 50 rain events of various types, recorded in 2007 and 2008, have been selected. They have been chosen during winter or summer, from high intensity (more than 30 mm/event) to low intensity. Each event lasts 24h and regroups periods with and without rain.

3. PRELIMINARY STUDIES, METHODOLOGY

3.1 Identification of the precipitation type of each radar pixel

The aim is to identify the precipitation type falling on each radar pixel and then to separate radar pixels into 3 groups: convective, stratiform and mixed.

A preliminary identification between convective and stratiform pixels has been carried out. Steiner *et al.* (1995) proposed an approach for identifying convective precipitation using three criteria but only the first two criteria have been used in this study since they were shown to be complementary and giving good results (Delrieu *et al.*, 2009). The first one consists on a reflectivity threshold: a pixel with reflectivity higher than 40 dBZ can be considered as convective, since rain of this intensity could practically never be stratiform. The second one looks for horizontal gradients: a pixel is assumed to be convective as soon as its reflectivity value exceeds the average reflectivity determined over a surrounding region (11 km radius circle centered on the pixel) from a given reflectivity difference (measured in dBZ). The identification of stratiform pixels has been based on the detection of a bright band (BB). Stratiform events are characterized by VPR with a high intensity pick which attests the presence of a BB whereas convective events are bereft (this information was supplied by Météo France).

The final separation into 3 groups has been done thanks to a tree decision: 1-convective pixel (according to Steiner) with no BB belonged to the convective group; 2- not convective pixel (according to Steiner) but with a BB belonged to the stratiform group; 3- the mixed group contains all the other pixels.

3.2 Methodology

Rain gauge data is taken as reference data. Each rain gauge data is compared to the radar data of the pixel containing the rain gauge. Results are studied through the analysis of 3 statistical scores: the Bias, the Mean Absolute Error (MAE) and the determination coefficient ($r^2 = r^2$). The Bias indicates if the radar tends to overestimate (positive Bias) or underestimate rainfall in comparison to the rain gauge (the optimal value being zero). MAE is here expressed in function of the mean precipitation

measured by the rain gauge. Finally r^2 is representative of data co-fluctuation.

$$Bias = \frac{\sum_{i=1}^n Ri - \sum_{i=1}^n Pi}{\sum_{i=1}^n Pi}, \quad (2)$$

$$MAE = \frac{\frac{1}{n} \sum_{i=1}^n |Ri - Pi|}{Pm},$$

$$r = \frac{\sum_{i=1}^n [(Pi - Pm) * (Ri - Rm)]}{\sqrt{\sum_{i=1}^n (Pi - Pm)^2} \sqrt{\sum_{i=1}^n (Ri - Rm)^2}},$$

where P_i and R_i are respectively rain gauge and radar data at the considered time step, n is the number of studied data and P_m is the mean precipitation measured by the rain gauge.

4. RAIN GAUGE / RADAR COMPARISON

4.1 Distance to the radar

The rain gauges have been gathered in 7 classes: 0-30 km, 30-45 km, 45-60 km, 60-70 km, 70-80 km, 80-100 km and higher than 100 km. Each class contains all the data of the rain gauges belonging to the class and their associated radar pixel. For each class and for each time step (5, 15, 30 and 60 min) the 3 statistical scores (Bias, MAE and r^2) have been computed (Figure 1). Results are significantly better with increasing time step: MAE decreases while r^2 increases. MAE decreases from 1.05 to 0.58 and r^2 increases from 0.2 to 0.58 (for respectively $\Delta t=5\text{min}$ and $\Delta t=60\text{min}$). The deterioration of those two scores correlated with the time step decreasing illustrates well the representativeness problem important for small time steps. If the Bias is independent of the time step it is dependent on the distance. With increasing distances and compared to rain gauges, the weather radar changes from an overestimation to an underestimation of rainfall. The 2 other scores seem to be not correlated to the distance and therefore are difficult to analyse. In this way, those results are surprising because we could have attended to a degradation of results with increasing distance.

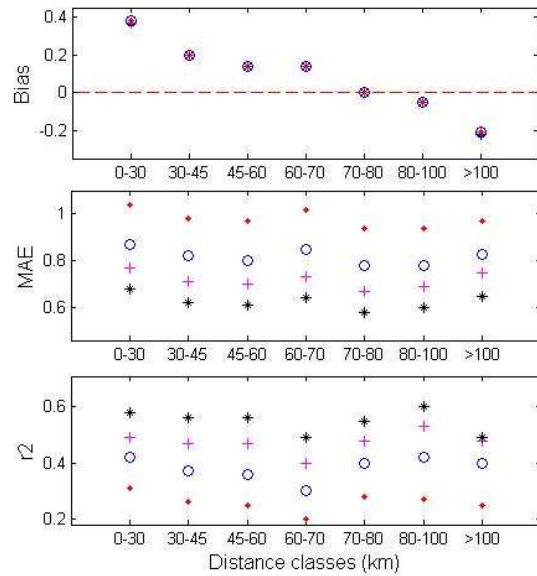


Figure 1 – Evolution of the Bias (above), the MAE (center) and the r^2 (below) computed between rain gauge and radar data in function of the distance from the radar and the time step: 5min (dots), 15min (circles), 30min (pluses) and 60min (stars).

4.2 Quality indicators

The same methodology has been applied but this time radar pixels, and their associated rain gauges, were separated in function of their quality indicators. The five following classes have been made: 76-84, 84-88, 88-92, 92-96 and 96-100. Lower quality indicators were not considered because too few pixels were concerned. Quality indicators being very dependent on distance, the five quality classes correspond globally to the following distance classes: higher than 100 km, 80-100 km, 60-80 km, 30-60 km and 0-30 km and thus this study did not give any new information.

4.3 Nature of the event

The same methodology has been applied by separating radar data into three classes: stratiform, convective and mixed (Figure 2). Better scores are obtained for stratiform pixels whatever the time step. R^2 reaches 0.7 for the stratiform group ($\Delta t=60\text{min}$) while it does not exceed 0.5 for the convective one.

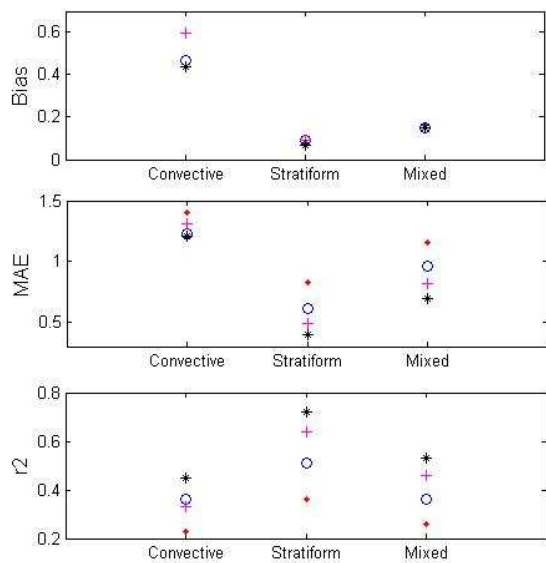


Figure 2 – Evolution of the Bias (above), the MAE (center) and the r^2 (below) computed between rain gauge and radar data in function of the nature of the event (convective, stratiform and mixed) and the time step: 5min (dots), 15min (circles), 30min (pluses) and 60min (stars).

To confirm or not those results the 50 events have been separated into two groups: the summer group (from April to September) and the winter group (from October to March). Each group contains all radar and rain gauge data measured during the considered period. Figure 3 shows the results for both groups in function of the distance and for the 60 minutes time step, knowing that the tendencies observed for this time step are the same whatever the time step. Results are significantly better in winter with a much higher r^2 and a MAE between 0.49 and 0.64 compared to a MAE ranging between 0.62-0.73 in summer. Those results are fully coherent with the previous ones: stratiform events predominate in winter and convective events in summer. It was noticed that in winter the determination coefficient strongly decreases with an increasing distance from the radar. This shows that during winter events VPR effects are more marked than in summer.

Those results are surprising because we could have thought that for stratiform (winter) events, characterised by a bright band, fluctuations between rain gauge and radar data would be the most important. No clear explanations have

been found. Maybe Z-R relationship in summer would be more varying and differ more from the Marshall-Palmer relationship (used in the processing chain) than in winter. Those results could also be due to attenuation and spatial variability more marked during convective (summer) events.

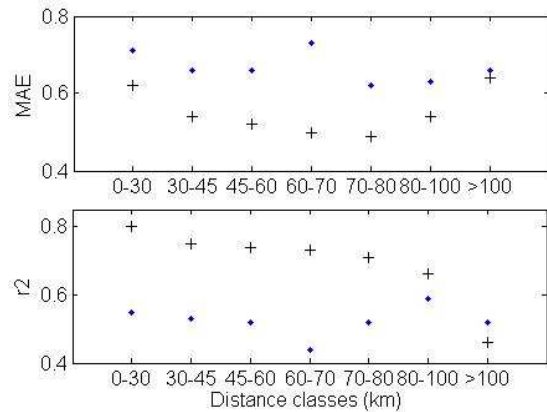


Figure 3 – Evolution of the MAE (above) and the r^2 (below) in function of the distance from the radar for summer events (dots) and winter events (pluses) for $\Delta t=60$ min.

4.4 Adjustment factor

The last step of the processing chain consists in applying an hourly adjustment factor to the radar image. Figure 4 shows the Bias and the r^2 evolution in function of the distance from the radar before and after the application of the factor for the 60 min time step. The tendencies observed are independent of the time step considered. The factor improves the results in a way that the co-fluctuation between rain gauge and radar data increases after the adjustment. It also reduced the Bias far from the radar but engenders an increase of the Bias close to the radar which becomes significant (equal to 0.4). Moreover we can note that before the adjustment the Bias is optimal close to the radar but deteriorates significantly with the distance from the radar increasing. This shows that range corrections are insufficient (no attenuation correction, VPR correction too cautious). In addition the adjustment method takes into account all rain gauges from 0 and 100 km around the radar. As the rain gauges density is

approximately homogeneous, rain gauges from 60 to 100 km are more in number than those from 0 to 60 km and therefore influence more the adjustment. This could explain why the bias becomes optimal for the 70-80 km class after the adjustment. So, the adjustment factor being the same for the entire radar image, a significant bias appears close to the radar after the adjustment.

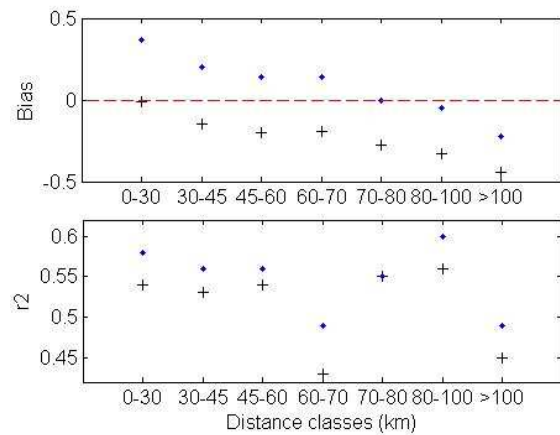


Figure 4 – Evolution of the Bias (above) and the r^2 (below) in function of the distance from the radar before (pluses) and after (dots) the adjustment method for $\Delta t=60$ min.

5. ACCURACY OF THE REFERENCE DATA

The present analysis considers the errors inherent to rain gauges and particularly the instrumental and the representativeness errors. An area rainfall at the radar pixel scale can be written as:

$$R_a = R_p + e_m + e_r, \quad (3)$$

where R_a is the area rainfall (radar rainfall), R_p the punctual rainfall measured by a rain gauge located inside the radar pixel, e_m the instrumental error and e_r the representativeness error. Those errors are assumed to be unbiased and independent which allows the characterization of the standard deviation of the total error (σ_{tot}) due to the rain gauge measurement of the rainfall at the radar pixel scale by:

$$\sigma_{tot}^2 = \sigma_m^2 + \sigma_r^2, \quad (4)$$

where σ_m and σ_r are respectively the standard deviation of the instrumental and the representativeness errors.

5.1 Instrumental error

Thanks to the analysis of 15 collocated rain gauges measurements, Ciach (2003) investigated the dependences of the instrumental error (named 'local random error') on rainfall intensity and timescale. He has shown that the standard deviation of this error (σ_m) can be expressed in function of those two variables using the following formula:

$$\sigma_m(T, R_p) = e_o(T) + R_o(T)/R_p, \quad (5)$$

where R_p is the rain gauge rain rate in mm/h, e_o and R_o are function of the time step T .

5.2 Representativeness error

Representativeness error is due to the fact that the rain gauge is a point and not an area measurement. The difference between area and point data is usually known as regularization (Journel and Huijbregts, 1978). The available data do not enable to determine the spatial structure of the rainfall at very small scales (Ciach and Krajewski, 2006). In order to obtain an order of magnitude of the representativeness error, we have used two sets of 3 equidistant rain gauges (respectively of 0.5 km and 1.5 km) measuring rainfall on two small urban catchments (equivalent to pixels): one of $0.5 \times 0.5 \text{ km}^2$ and one of $1.5 \times 1.5 \text{ km}^2$. The area rainfall (R_a) over a pixel is estimated by the average value of the 3 rain gauges. The observations with equal average values have been assumed to belong to the same population characterized by its standard deviation. This standard deviation is assumed representative of the representativeness error associated with this average value. The experimental data regroups one year of continuous rainfall measurement. For each time step and for both case ($0.5 \times 0.5 \text{ km}^2$ and $1.5 \times 1.5 \text{ km}^2$), we have plotted the computed standard deviation against average rain rates values (R_a) (Figure 5 for $\Delta t=5$ min). It appears acceptable to deduce a linear relation between the standard deviation of the representativeness error (σ_r) and the rain rates (R_a). Relations between both variables in our case ($1 \times 1 \text{ km}^2$) were obtained by combining the results of the $0.5 \times 0.5 \text{ km}^2$ and $1.5 \times 1.5 \text{ km}^2$ cases (Figure 5 and equations 6).

$$\sigma_r (\Delta t=5\text{min}, R_a) = 0.0485 * R_a, \quad (6)$$

$$\sigma_r (\Delta t=15\text{min}, R_a) = 0.0292 * R_a,$$

$$\sigma_r (\Delta t=30\text{min}, R_a) = 0.0213 * R_a,$$

$$\sigma_r (\Delta t=60\text{min}, R_a) = 0.0136 * R_a,$$

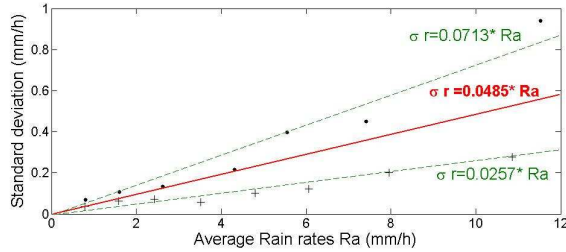


Figure 5 – Standard deviations of the representativeness errors as function of the rainfall intensities for $\Delta t=5\text{min}$, for the $1.5 \times 1.5 \text{ km}^2$ (dots) and $0.5 \times 0.5 \text{ km}^2$ (pluses) case. The dashed lines represent their linear fit. The linear fit at $1 \times 1 \text{ km}^2$ is represented by the solid line.

5.3 New comparison rain gauge /radar data

The quality of the reference data is taken into account through its estimated standard deviation (σ_{tot}). One may consider that the radar measurement is not statistically different from the rain gauge value at a given significance level if it is included in the corresponding confidence interval. The criterion considered is the percentage of radar measurements included within the confidence interval at 68% (written PC68, equation 7). If this proportion reaches 68%, it can be accepted that there is no significant statistical difference between ground and radar data.

$$\text{PC68} = [R_p - \sigma_{\text{tot}}, R_p + \sigma_{\text{tot}}], \quad (7)$$

with R_p is the rain gauge rain rates in mm/h and σ_{tot} the standard deviation of the total error in mm/h (equation 4).

The percentages of values within the confidence interval are for the four time steps (5, 15, 30, 60 min) respectively of 91%, 75%, 56% and 43%. The percentages at $\Delta t=5\text{min}$ and 15min are high. This can be explained by the fact that the total standard deviations for those time steps are

very important, therefore the confidence interval is very large. For such small time steps rain gauge data is not totally representative of rainfall over a pixel. With the time step increasing, the standard deviations reduced and rain gauge data becomes reliable. In this case the statistical difference between radar measurements and ground is significant.

6. CONCLUSION

The objective of this work was to evaluate, for urban time steps (5, 15, 30 and 60 min), the French new operational radar product developed by Météo France. In Paris area during 50 varied events, the comparison between rain gauge and radar data has shown that for small time steps (5 and 15 min) rain gauge data is not fully representative of rainfall over a pixel. So, it is not easy to conclude on the quality of the radar data. For higher time steps (30 and 60 min) rain gauge data is accurate. In this case radar data differs from rain gauge data. This difference is mostly due to the existence of a high bias between both data, their co-fluctuation being relatively satisfactory. This significant bias close to the radar seems to be a consequence of the adjustment method. So, and in our context, the use of radar data for an urban hydrological study requires beforehand a new local adjustment between radar and rain gauges. This adjustment is particularly necessary near the radar and during convective events.

7. ACKNOWLEDGMENTS

This work would not have been possible without the contribution of Claudine Gueguen who extracted and helped us to read all the radar and rain gauge data, many thanks!

8. REFERENCES

- Ciach, G.J., 2003: Local random errors in Tipping-Bucket rain gauge measurements. *Journal of Atmospheric and Oceanic Technology*, 20, 752-9.
- Ciach, G.J., and Krajewski, W.F., 2006: Analysis and modeling of spatial correlation structure in small-scale rainfall in Central Oklahoma. *Advances in Water Resources*, 29, 1450-1463.
- Delrieu, G., Boudevillain, B., Nicol, J., Chapon, B., Kirstetter, E., Andrieu, H. and Faure, D., 2009: Bollène-2002 Experiment: Radar Quantitative Precipitation Estimation in the

Cévennes-Vivarais Region, France. *Journal of Applied Meteorology and Climatology*, 48, 1422-1447.

Journel, A.G., and Huijbregts, C.J., 1978: *Mining Geostatistics*, Academic Press, London.

Steiner, M., Houze, R.A., and Yuter, S.E., 1995: Characterization of three dimensional storm structure from operational radar and rain gauge data. *Journal of Applied Meteorology*, 34, 1978-2007.

Tabary, P., 2007: The new French operational radar rainfall product. Part 1: methodology. *Weather and Forecasting*, 22, 393-408.

Tabary, P., Desplats, J., Do Khac, K., Eideliman, F., Guégen, C., and Heinrich, J.C., 2007: The new French operational radar rainfall product. Part 2: validation. *Weather and Forecasting*, 22, 409-427.